Increasing Quantum Efficiency of Polymer Solar Cells with Efficient Exciton Splitting and Long Carrier Lifetime by Molecular Doping at Heterojunctions

Han Yan,[*,†] Yabing Tang,[†] Xinyu Sui,[‡] Yucheng Liu,[§] Bowei Gao,[∥] Xinfeng Liu,[‡] Shengzhong(Frank) Liu,[§] Jianhui Hou,[∥] and Wei Ma[*,†]

[†] State Key Laboratory for Mechanical Behavior of Materials, Xi'an Jiaotong University, Xi'an 710049, P. R. China

[‡] Division of Nanophotonics; CAS Key Laboratory of Standardization and Measurement for Nanotechnology; CAS Center for Excellence in Nanoscience; National Center for Nanoscience and Technology, Beijing 100191, P. R. China

[§] Key Laboratory of Applied Surface and Colloid Chemistry, National Ministry of Education; Shaanxi Key Laboratory for Advanced Energy Devices; Shaanxi Engineering Lab for Advanced Energy Technology; Institute for Advanced Energy Materials; School of Materials Science and Engineering, Shaanxi Normal University, Xi'an 710119, P. R. China

[∥] State Key Laboratory of Polymer Physics and Chemistry; Beijing National Laboratory for Molecular Sciences; CAS Research/Education Center for Excellence in Molecular Sciences; Institute of Chemistry, Chinese Academy of Sciences, Beijing 100049, P. R. China

Corresponding Author

* E-mail: mseyanhan@xjtu.edu.cn (H. Yan.); msewma@xjtu.edu.cn (W. Ma)

Experimental Section

Materials: PBDB-T and ITIC were purchased from Solarmer Materials Inc. BCF, zinc acetate dihydrate, ethanolamine, and 2-methoxyethanol were purchased from Sigma-Aldrich. All chemicals in the experiments were used as received.

Instrumentation: The J-V curves were measured in the N_2 glovebox under AM 1.5G (100 mW/cm^2) using an AAA solar simulator (SS-F5-3A, Enli Technology Co., Ltd.) calibrated with a standard photovoltaic cell equipped with KG5 filter and a Keithley 2400 source meter. Typical cells have device areas of 4 mm^2, defined by a mask with aperture aligned with the device area. The EQE was measured by Solar Cell Spectral Response Measurement System QE-R3018 (Enli Technology Co., Ltd.). The light intensity was calibrated with a standard Si photovoltaic cell. The absorption spectra were acquired on a Shimadzu UV-3600 Plus. The thickness of active layer was measured by Bruker Dektak XT. Femtosecond transient absorption measurements were carried out with a temporal resolution of ~120 fs t on a commercial femtosecond TAS system (HELIOS, Ultrafast Systems). Briefly, the fundamental 800 nm pulse from a regenerative amplifier (80 fs, 1 kHz, 2.5 mJ per pulse, Coherent, Astrella), seeded by a oscillator (35 fs, 80 MHz, Coherent Vitara-S), was used to pump an optical parametric amplifier (Coherent, OperA Solo) to generate excitation pulse peaking at 400 nm. The pump beam was chopped by 500 Hz in order to get the shot to shot measurement. The pump fluence was attenuated to ~10 μJ cm^{-2} with two variable neutral density filter .The probe light was get where a small fraction of the 800 nm output from the Astrella was fed to a sapphire crystal in the HELIOS for

generating the white light continuum (WLC). Steady and time-resolved PL measurements were taken using a PicoQuant FT-300 and FT-100 with different excitation wavelength. UPS spectrum was collected on ESCALAB Xi+ (Thermo Fisher). The TPV measurements were performed by the all-in-one characterization platform Paios developed and commercialized by Fluxim AG, Switzerland

Device Fabrication: The invertd PSCs were fabricated with a configuration of ITO/ZnO/Active Layer/MoO_3/Ag. The normal PSCs were fabricated with a configuration of ITO/PEDOT:PSS/Active Layer/Ca/Al. The ITO substrates were cleaned by sequential sonication in deionized water, acetone and isopropanol for 20 min of each step. After UVO treatment for 20 min, and electron-transporting layer of ZnO was deposited by spin-coating a ZnO precursor solution (dissolving zinc acetate in 2-methoxyethanol with ethanolamine) at 4500 rpm for 40s, followed by thermal annealing at 200 ℃ for 30 min. The hole-transporting layer of PEDOT:PSS was deposited by spin-coating at 4500 rpm for 40s, followed by thermal annealing at 150 ℃ for 10 min. PHJ devices were fabricated by floating-film-transfer method, which was used to stack the PBDB-T layer on the ITIC layer. The PBDB-T film was floated in water, and then it was scooped up by ITIC coated cathode substrate. BHJ devices were fabricated by spin-coating PBDB-T/ITIC blend solution or sequentially spin-coating each single component with different processing conditions in the N_2 glove box. Finally, 10 nm MoO_3 / 100 nm Ag or 20 nm Ca / 80 nm Al were sequentially deposited as the anode or cathode at a vacuum level of $< 1\times10^{-4}$ Pa.

GIWAXS characterization: GIWAXS measurements were performed at beamline 7.3.3 at the Advanced Light Source (ALS). Samples were prepared on Si substrates using identical blend solutions as those used in devices. The 10 keV X-ray beam was incident at a grazing angle of 0.12-0.16°, selected to maximize the scattering intensity from the samples. The scattered X-ray were detected using a Dectris Pilatus 2M photon counting detector.

TAS lifetime:

The TAS decay signals are fitted using a Gaussian response function convoluted with multi-exponential decay function:

$$e^{-\frac{t^2}{\tau_{pulse}^2}} \otimes \sum A_i e^{-\frac{t}{\tau_i}}$$

and the TAS lifetime is further calculated according to the following equation:

$$\tau = \frac{\sum A_i \tau_i^2}{\sum A_i \tau_i}$$

Carrier lifetime calculation:

The carrier lifetime is calculated according to the TPV tests. In organic photovoltaics, the V_{oc} can be calculated by the following equation:

$$V_{oc} = \frac{E_g}{q} - \frac{n_{eff} k_B T}{q} \ln\left(\frac{N^2}{np}\right)$$

where E_g is the bandgap of organic photovoltaics, n_{eff} is the effective ideality factor, k_B is the Boltzmann's constant, T is the absolute temperature, q is the elemental charge, and n & p are the density of electrons and holes.

The V_{oc} decay is calculated by deriving the upper equation:

$$q\frac{dV_{oc}}{dt} = k_B T\frac{dln(np)}{dt}$$

Then the carrier lifetime is calculated from the TPV data:

$$\tau = -\frac{k_B T}{q}\left(\frac{dV_{oc}}{dt}\right)^{-1}$$

We have added these details in the supporting information.

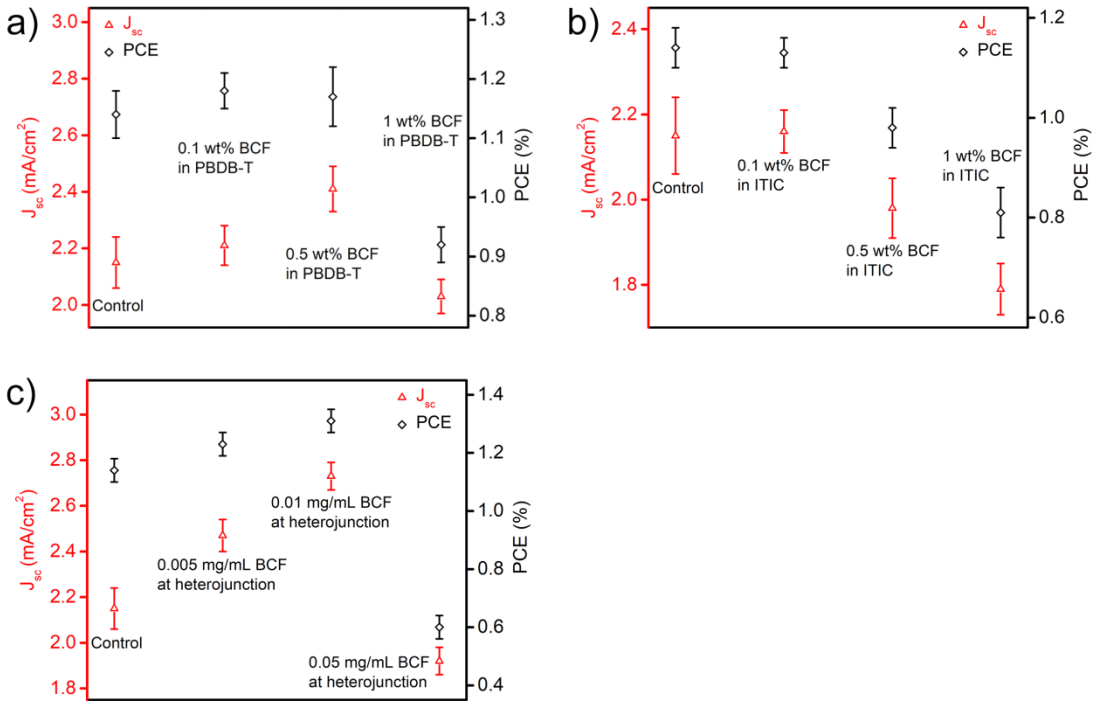

Figure S1. Plots of J_{sc} and PCE in PHJ device structure in accordance with Table 1.

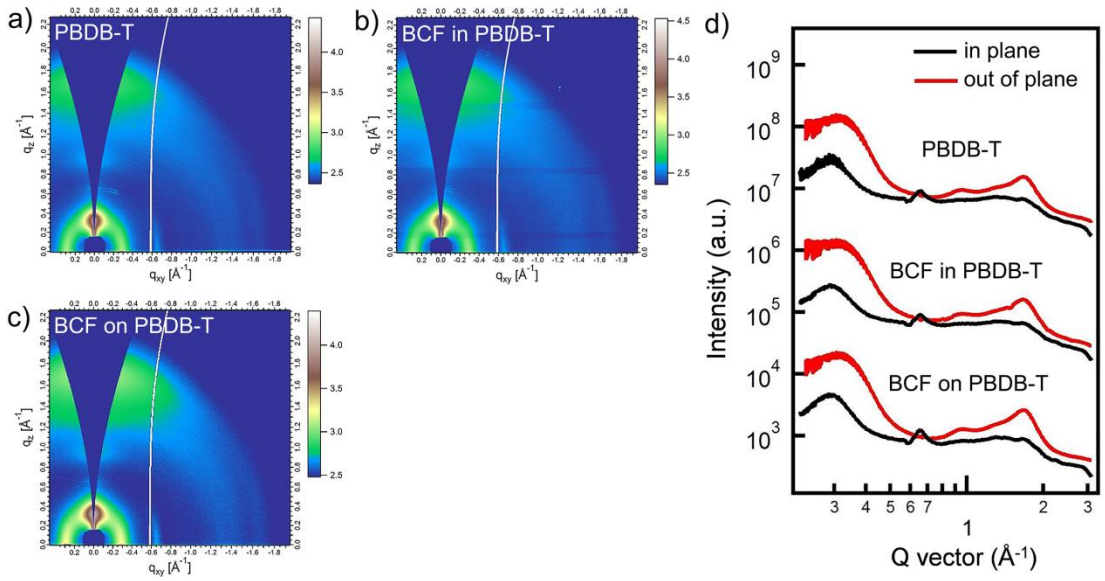

Figure S2. a-c) GIWAXS patterns of PBDB-T films: a) neat; b) 0.1 wt% BCF in PBDB-T; c) 0.01 mg/mL BCF on PBDB-T. d) Corresponding in plane and out of plane line cuts.

Table S1. The fitted peak position and coherence length from GIWAXS patterns for PBDB-T films.

Materials	Location (Å^{-1})	d-spacing (Å)	FWHM (Å^{-1})	CL (nm)
PBDB-T	0.29	21.66	0.086	6.55
BCF in PBDB-T	0.29	21.58	0.092	6.15
BCF on PBDB-T	0.29	21.64	0.093	6.11

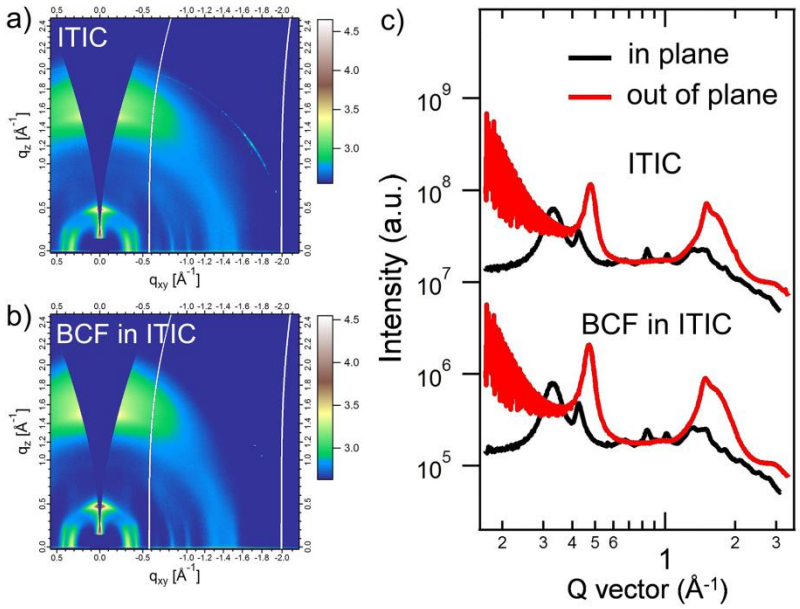

Figure S3. a, b) GIWAXS patterns of ITIC films: a) neat; b) 0.1 wt% BCF in ITIC. c) Corresponding in plane and out of plane line cuts.

Table S2. The fitted peak position and coherence length from GIWAXS patterns for ITIC films.

Materials	Location (Å^{-1})	d-spacing (Å)	FWHM (Å^{-1})	CL (nm)
ITIC	0.33	19.12	0.063	8.92
BCF in ITIC	0.33	19.11	0.064	8.83

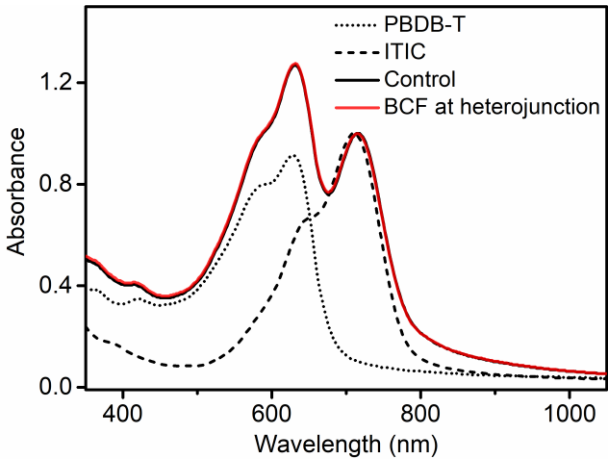

Figure S4. Steady absorption spectra of neat and PHJ films.

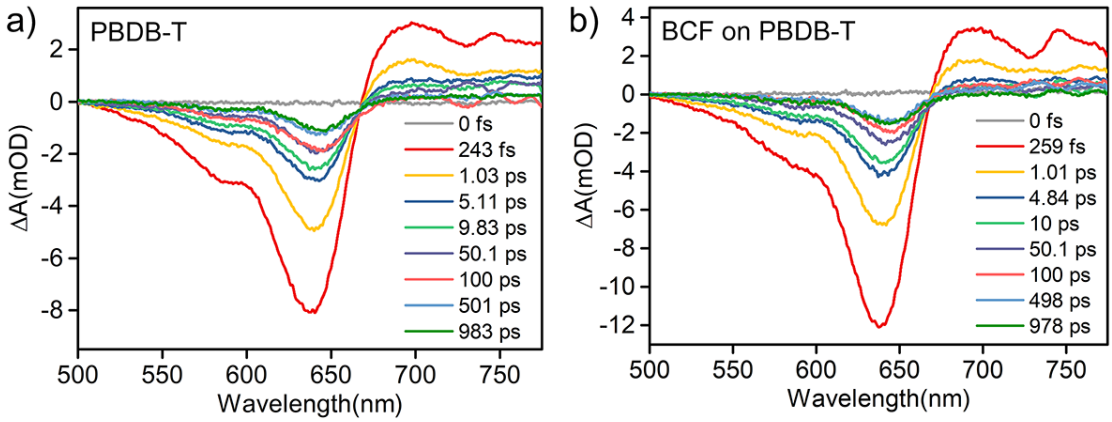

Figure S5. Transient absorption spectra of PBDB-T films using 400 nm laser pulse excitation: a) neat; b) BCF on PBDB-T.

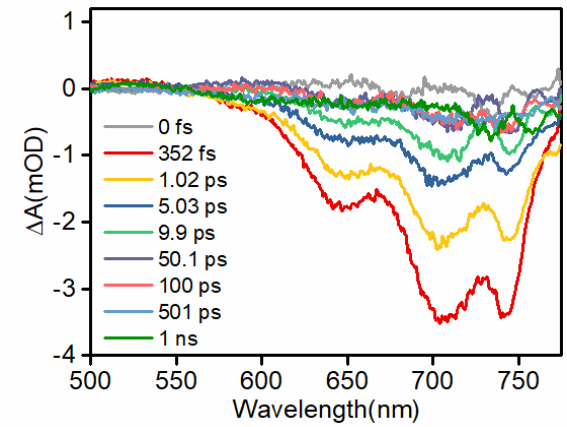

Figure S6. Transient absorption spectra of ITIC film using 400 nm laser pulse excitation.

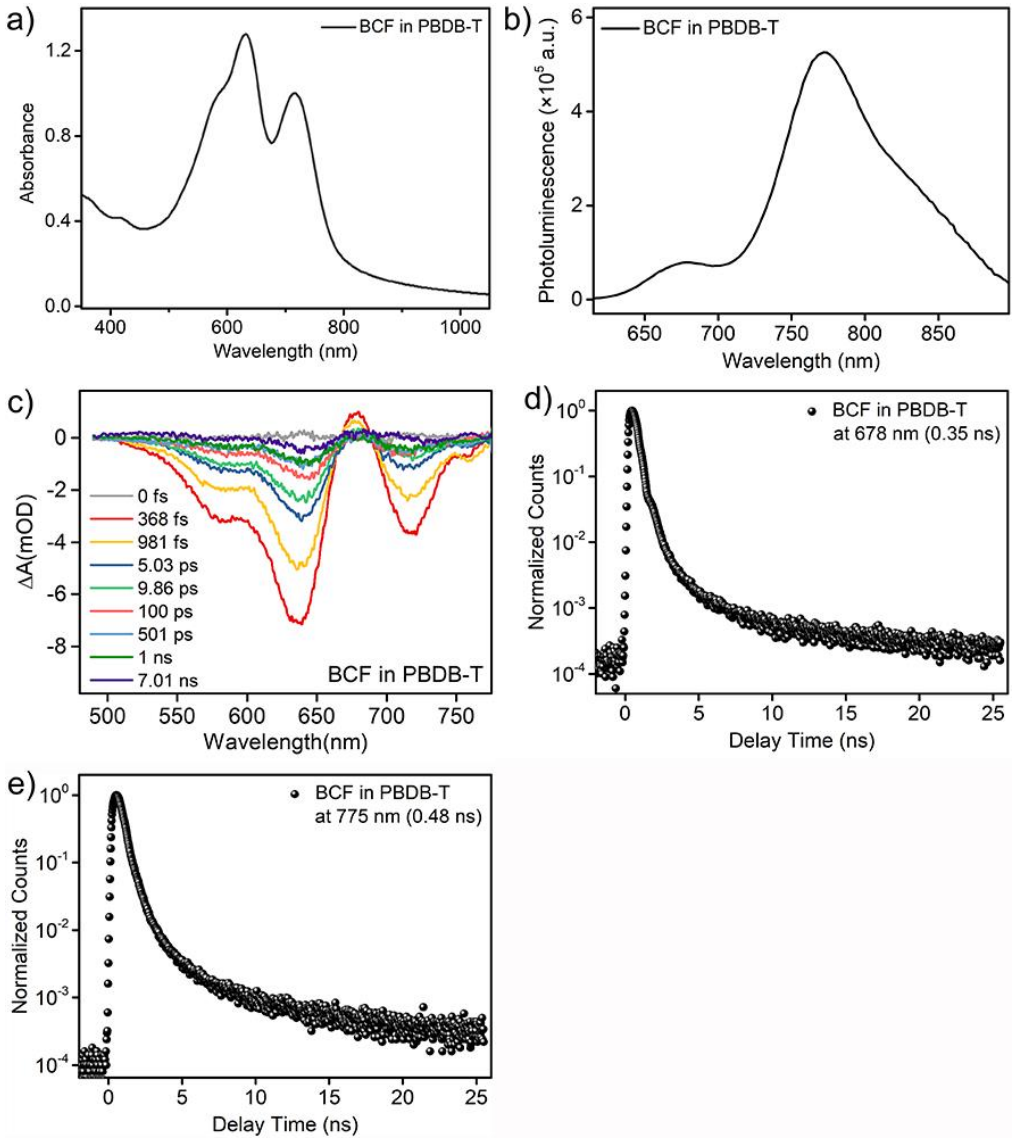

Figure S7. Spectral studies of 0.1 wt% BCF in PBDB-T: a) steady absorption spectra; b) steady state photoluminescence spectra recorded using 400 nm excitation; c) transient absorption spectra using 400 nm laser pulse excitation; d and e) transient PL spectra probing the peak at 678 nm and 775 nm.

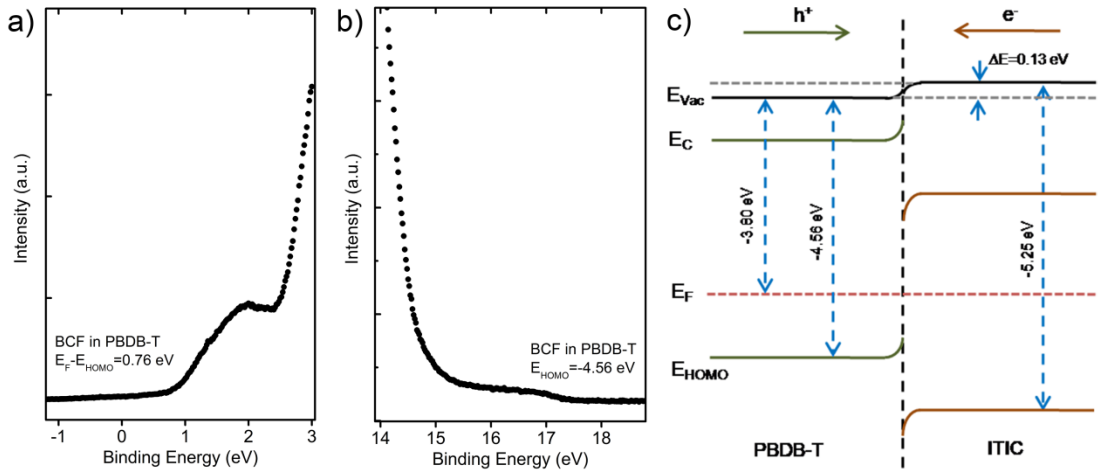

Figure S8. UPS spectra of the 0.1 wt% BCF in PBDB-T film under -10 V bias: a) low and b) high energy part of PBDB-T films. c) The scheme of band diagrams according to the UPS spectra.

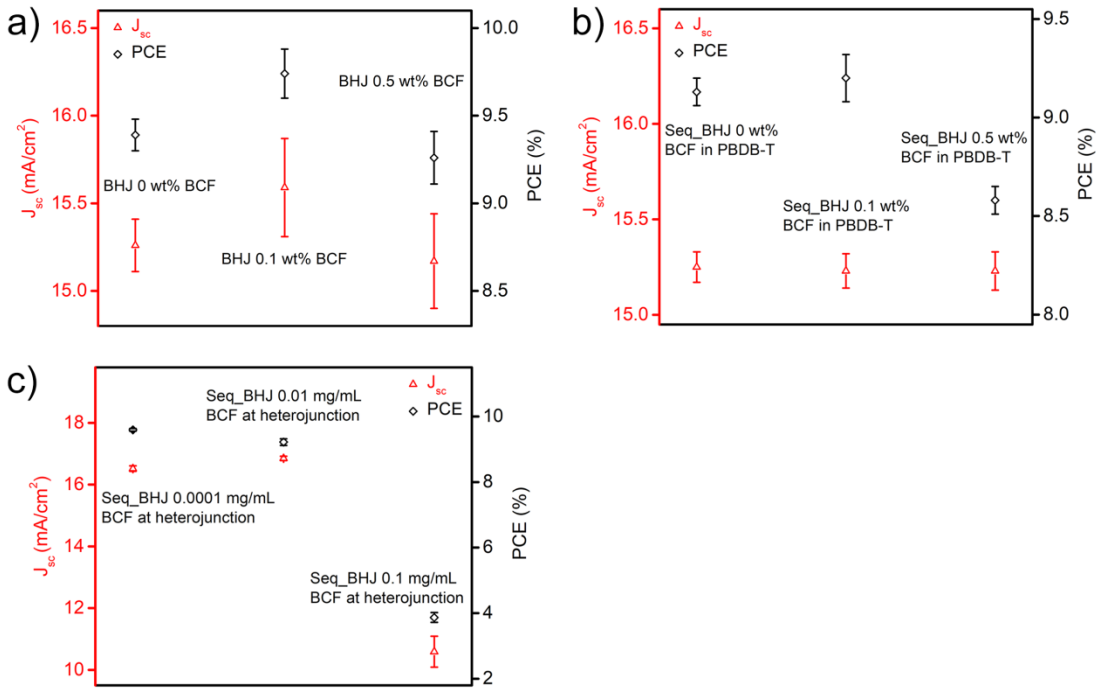

Figure S9. Plots of J_{sc} and PCE under various fabricating processes in accordance with Table 2.

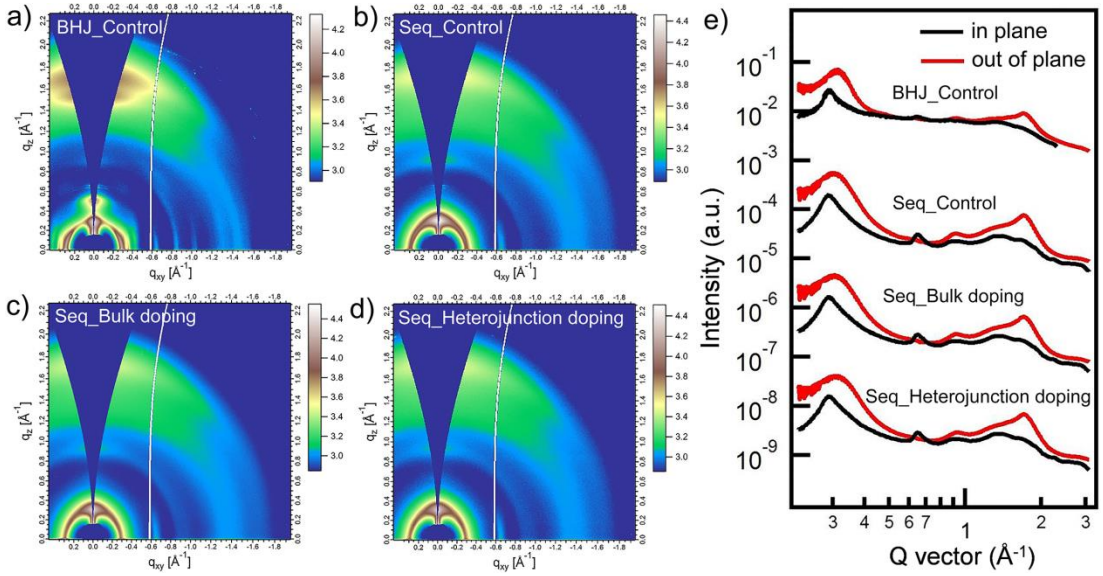

Figure S10. a-c) GIWAXS patterns of BHJ films: a) conventional BHJ; b) sequential spin-coating BHJ; c) sequential spin-coating 0.1 wt% BCF doped BHJ; d) sequential spin-coating 0.01 mg/mL BCF interfacial doped BHJ. e) Corresponding in plane and out of plane line cuts.

Table S3. The fitted peak position and coherence length from GIWAXS for BHJ films.

Materials	Location (Å^{-1})	d-spacing (Å)	FWHM (Å^{-1})	CL (nm)
BHJ_Control	0.29	21.64	0.028	20.05
Seq_Control	0.29	21.79	0.035	16.05
Seq_Bulk doping	0.29	21.62	0.042	13.55
Seq_Heterojunction doping	0.29	21.59	0.040	14.00